

Testing the viability of the interacting holographic dark energy model by using combined observational constraints

Chang Feng and Bin Wang*

Department of Physics, Fudan University, 200433 Shanghai

Yungui Gong[†]

*School of Physical Science and Technology,
Southwest University, Chongqing 400715, China*

Ru-Keng Su[‡]

*China Center of Advanced Science and Technology (World Laboratory) P.O. Box 8730,
100080 Beijing and Department of Physics,
Fudan University, Shanghai 200433, China*

Abstract

Using the data coming from the new 182 Gold type Ia supernova samples, the shift parameter of the Cosmic Microwave Background given by the three-year Wilkinson Microwave Anisotropy Probe observations, and the baryon acoustic oscillation measurement from the Sloan Digital Sky Survey, $H(z)$ and lookback time measurements, we have performed a statistical joint analysis of the interacting holographic dark energy model. Consistent parameter estimations show us that the interacting holographic dark energy model is a viable candidate to explain the observed acceleration of our universe.

PACS numbers: 98.80.Cq; 98.80.-k

*Electronic address: wangb@fudan.edu.cn

[†]Electronic address: yungui.gong@baylor.edu

[‡]Electronic address: rksu@fudan.ac.cn

The present continuous flow of cosmological data provides us day by day a clearer picture that our universe is experiencing accelerated expansion [1]. In order to draw precise conclusions from the available phenomenological perspectives on how fast the universe is expanding at present, how long this speed up has lasted and how the acceleration rate has changed over the recent past, we have to overcome statistical uncertainties and possible theoretical biasing in the tests used. This requires us to refine the existing tests and devise new ones.

Recently Simon et al [2] have published Hubble parameter data extracted from differential ages of passively evolving galaxies. It is interesting to use these data to constrain the evolution of the universe. This is so because that they can provide consistent checks and tight constraints on models when combined with other cosmological tests, and also because the Hubble parameter is not integrated over like that of the luminosity distance and it can give better constraints on the cosmological parameters. Recently, Hubble parameter data have been used to constrain several cosmological models [3, 4].

To reduce the degeneracy in viable candidate cosmological models designed to explain the observed accelerated expansion, new observables should be added to the usual ones. Recalling that the test of cosmological models by the type Ia supernova (SN Ia) data is a distance based method, it is of interest to look for tests based on time-dependent observable. In [5, 6], the age of an old high redshift galaxy has been used to constrain the model. To overcome the problem that the estimate of the age of a single galaxy maybe affected by systematic errors, it is needed to consider a sample of galaxies belonging to the same cluster. Recently, the age estimates of around 160 galaxy clusters at six redshifts distributed in the interval $0.10 < z < 1.27$ have been compiled by Capozziello et al [7]. Employing these data, one can take into account the lookback time which was defined by Sandage [8] as the difference between the present age of the universe and its age when a particular light ray at redshift z was emitted. This quantity can discriminate among different cosmological models. The lookback time has been used as a test for some cosmological models [7, 9].

In this paper we will use the latest SN Ia data compiled by Riess et al [10], the Cosmic Microwave Background (CMB) shift parameter derived from the three-year Wilkinson Microwave Anisotropy Probe (WMAP3) observations [11], the baryon acoustic oscillations (BAO) measurement from the large-scale correlation function of the Sloan Digital Sky Survey (SDSS) luminous red galaxies [12] in combination with the $H(z)$ data and the lookback time data to give a complete investigation on the viability of the interacting holographic dark energy model devised in [13]. Recently, this model has confronted the tests from the SN Ia data [13], the age constraint and the small l CMB spectrum constraint [6]. It has been argued that the interacting holographic dark energy model can

accommodate the transition of the dark energy equation of state w from $w > -1$ to $w < -1$ [13, 14], as recently revealed from extensive data analysis [15]. With the interaction between dark energy and dark matter introduced in [13], it has been shown that the old astrophysical structures can be formed naturally [6] and the coincidence problem can be alleviated [6, 16]. The thermodynamical properties of the universe with the interacting holographic dark energy have also been studied [17]. Very recently, the combined constraint on the interacting holographic dark energy model using the SN Ia data, the BAO measurement and the shift parameter determined from the SDSS and WMAP3 has been reported [18]. This paper aims to place combined new observational constraints on this interacting holographic dark energy model by including the Hubble parameter data and the lookback time data. Different from the distance based test, the lookback time is a time based method. Moreover, the Hubble parameter does not suffer the integration effect in the luminosity distance. It is expected that these new tests will further constrain the model.

Recently, inspired by the holographic hypothesis [19], a new model has been put forward to explain the dark energy. The energy density cannot exceed the mass of a black hole with the same size of the universe L , thus we have $\rho_D = 3c^2L^{-2}$, where c is a constant and the Planck mass M_p has been taken unity. Choosing L as the future event horizon, $R_h = a \int_a^\infty \frac{da}{Ha^2}$, we have $\rho_D = 3c^2R_h^{-2}$ as the dark energy density. As far as energy conservation is concerned, we suppose that the interaction is described by the (separately non conserving) equations

$$\dot{\rho}_m + 3H\rho_m = Q \quad (1)$$

$$\dot{\rho}_D + 3H(1 + \omega_D) = -Q \quad (2)$$

where Q is some interaction term. For the moment we take for granted that the interaction is the one proposed on general grounds in [20], which is $Q = 3b^2H(\rho_m + \rho_D)$, where b^2 is the second phenomenological constant indicating coupling between dark energy and dark matter. Positive values of b^2 would correspond to a transfer of energy from the dark energy to dark matter, while the negative b^2 would imply a transfer of energy from the dark matter to the dark energy [21]. In view of the unknown nature of dark matter and dark energy, we do not put any limit on the sign of b^2 at first and wait to determine it from the observational data. Because of the interaction, neither dark energy nor dark matter conserve whence they evolve separately. For the flat universe, using the Friedmann equation $\Omega_D + \Omega_m = 1$, where $\Omega_D = \frac{\rho_D}{3H^2}$ and $\Omega_m = \frac{\rho_m}{3H^2}$, the evolution behavior of the dark energy was obtained as [13]:

$$\frac{\Omega'_D}{\Omega_D^2} = (1 - \Omega_D) \left[\frac{2}{c\sqrt{\Omega_D}} + \frac{1}{\Omega_D} - \frac{3b^2}{\Omega_D(1 - \Omega_D)} \right]. \quad (3)$$

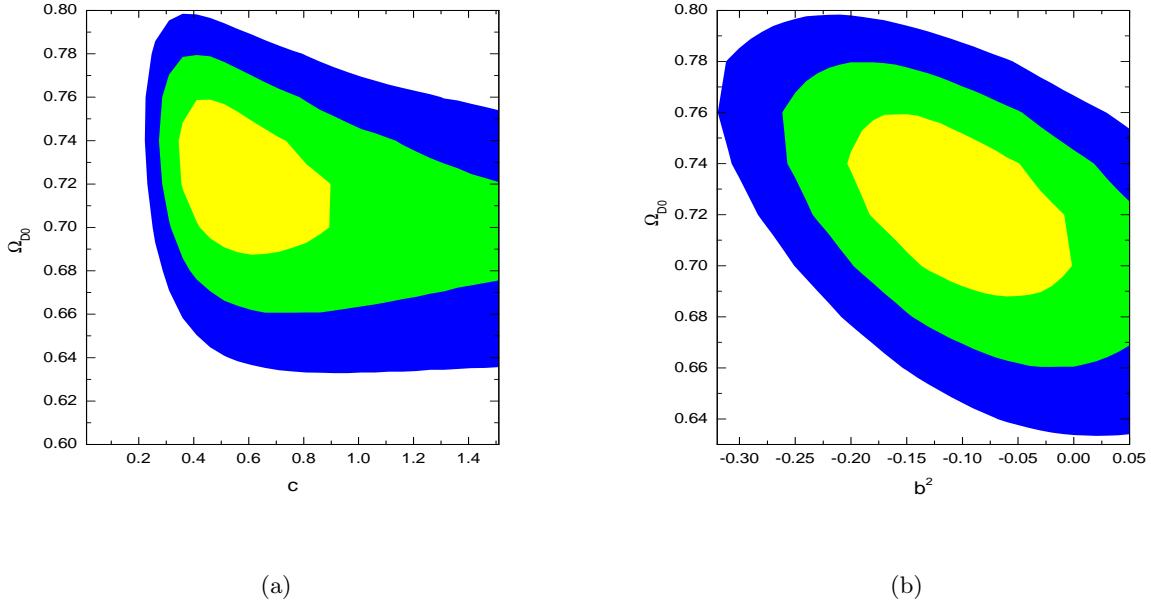


Figure 1: (a) The contours from the combination of SN Ia, BAO in the interacting holographic dark energy model for c and Ω_{D0} at 1σ , 2σ , 3σ confidence level with $b^2 = -0.10$. (b) The contours from the combination of SN Ia, BAO for b^2 and Ω_{D0} at 1σ , 2σ , 3σ confidence level with $c = 0.53$.

The prime denotes the derivative with respect to $x = \ln a$. The equation of state of dark energy was expressed as [13]

$$\omega_D = -\frac{1}{3} - \frac{2\sqrt{\Omega_D}}{3c} - \frac{b^2}{\Omega_D}. \quad (4)$$

By suitably choosing the coupling between dark energy and dark matter, this model can accommodate the transition of the dark energy equation of state from $\omega_D > -1$ to $\omega_D < -1$ [13, 14], which is in agreement with the recent analysis of the SN Ia data [15]. The deceleration parameter has the form

$$q = \frac{1}{2} - \frac{3b^2}{2} - \frac{\Omega_D}{2} - \frac{\Omega_D^{3/2}}{c}. \quad (5)$$

The evolution of the Hubble parameter can be written as

$$H(z) = H_0 \exp \left[\int_0^z \frac{1+q'}{1+z'} dz' \right] \quad (6)$$

Next we constrain the interacting holographic dark energy model by using the latest observational data, such as the gold SN Ia data, the shift parameter and the BAO measurement from WMAP3 and SDSS, and combining these observations with $H(z)$ data and lookback time data.

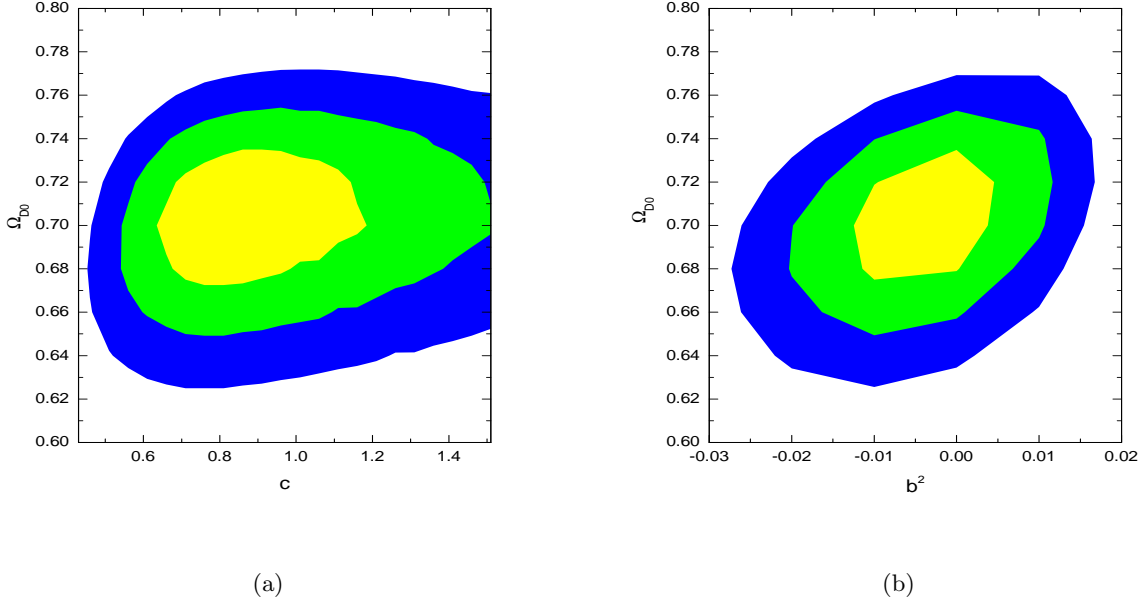


Figure 2: (a)The contours from the combination of SN Ia, BAO, CMB in the interacting holographic dark energy model for c and Ω_{D0} at 1σ , 2σ , 3σ confidence level with $b^2 = -0.004$. (b)The contours from the combination of SN Ia, BAO, CMB for b^2 and Ω_{D0} at 1σ , 2σ , 3σ confidence level with $c = 0.84$.

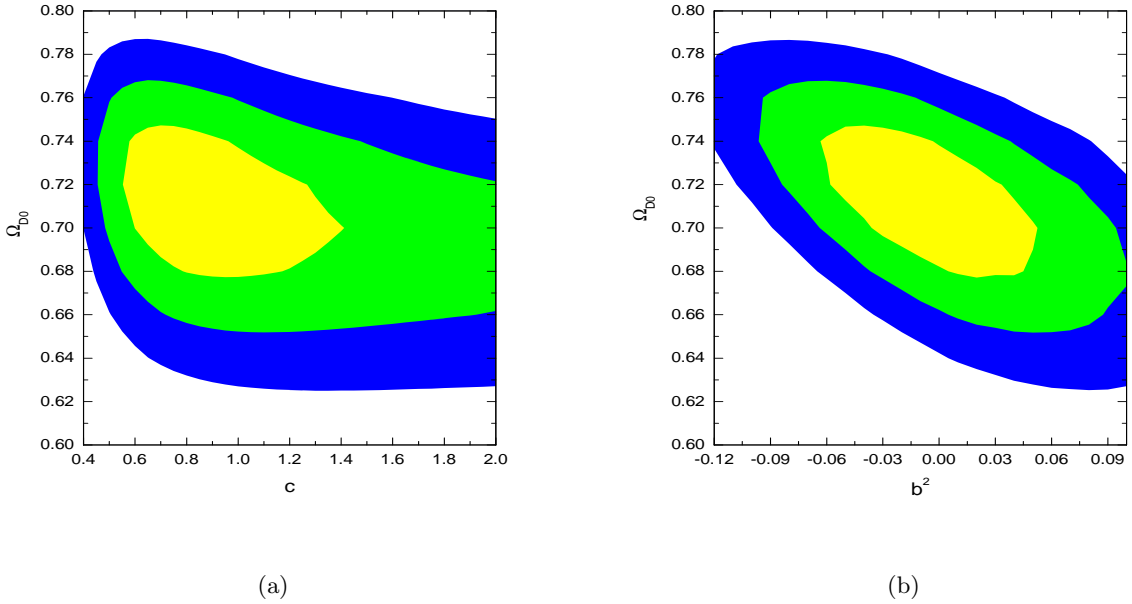


Figure 3: (a)The contours from the combination of SN Ia, BAO, $H(z)$ in the interacting holographic dark energy model for c and Ω_{D0} at 1σ , 2σ , 3σ confidence level with $b^2 = -0.005$. (b)The contours from the combination of SN Ia, BAO, $H(z)$ for b^2 and Ω_{D0} at 1σ , 2σ , 3σ confidence level with $c = 0.82$. We have employed $H_0 = 72 \text{ km} \cdot \text{s}^{-1} \cdot \text{Mpc}^{-1}$.

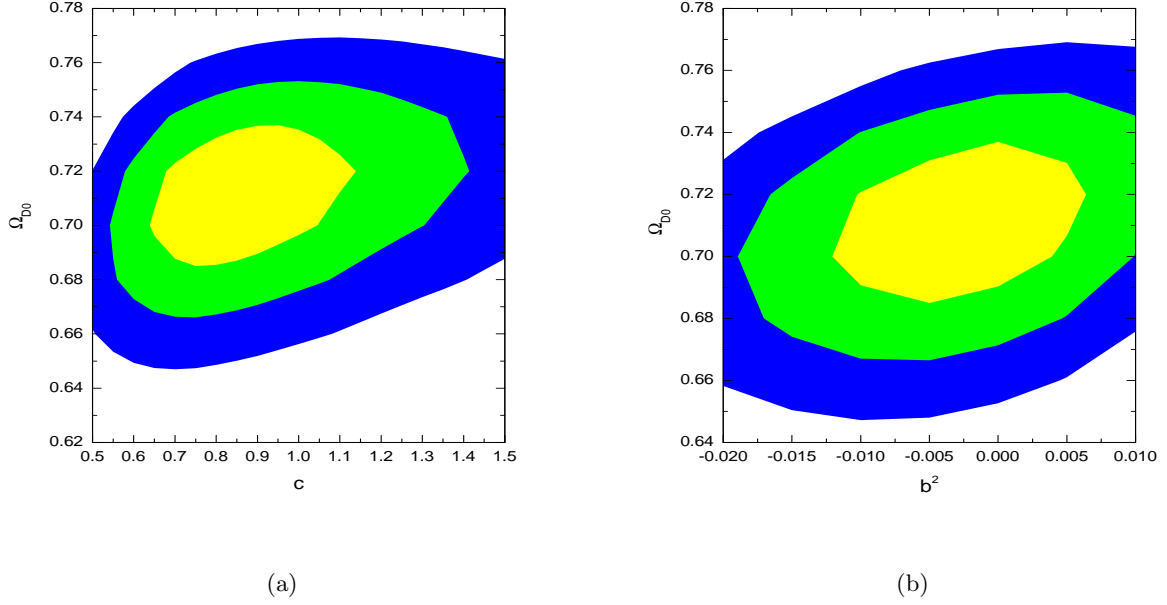


Figure 4: (a)The contours from the combination of SN Ia, BAO, $H(z)$, CMB in the interacting holographic dark energy model for c and Ω_{D0} at 1σ , 2σ , 3σ confidence level with $b^2 = -0.003$. (b)The contours from the combination of SN Ia ,BAO, $H(z)$, CMB for b^2 and Ω_{D0} at 1σ , 2σ , 3σ confidence level with $c = 0.84$. We have employed $H_0 = 72km \cdot s^{-1} \cdot Mpc^{-1}$.

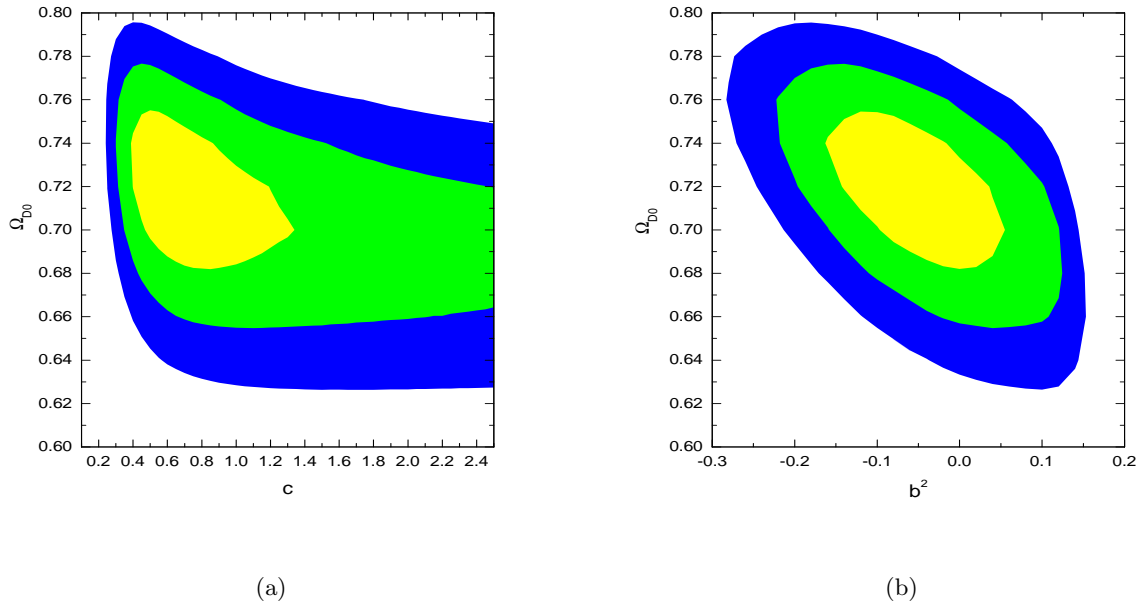


Figure 5: (a)The contours from the combination of SN Ia, BAO, Lookback time in the interacting holographic dark energy model for c and Ω_{D0} at 1σ , 2σ , 3σ confidence level with $b^2 = -0.059$. (b)The contours from the combination of SN Ia, BAO, Lookback time for b^2 and Ω_{D0} at 1σ , 2σ , 3σ confidence level with $c = 0.62$.

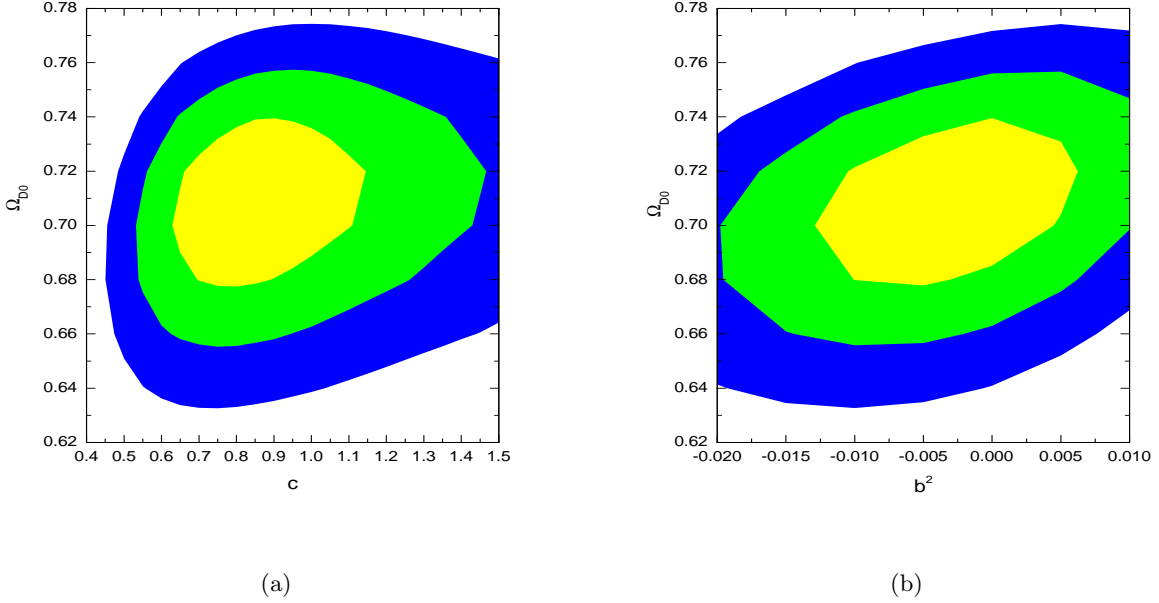


Figure 6: (a) The contours from the combination of SN Ia, BAO, Lookback time, CMB in the interacting holographic dark energy model for c and Ω_{D0} at 1σ , 2σ , 3σ confidence level with $b^2 = -0.003$. (b) The contours from the combination of SN Ia, BAO, Lookback time, CMB for b^2 and Ω_{D0} at 1σ , 2σ , 3σ confidence level with $c = 0.83$.

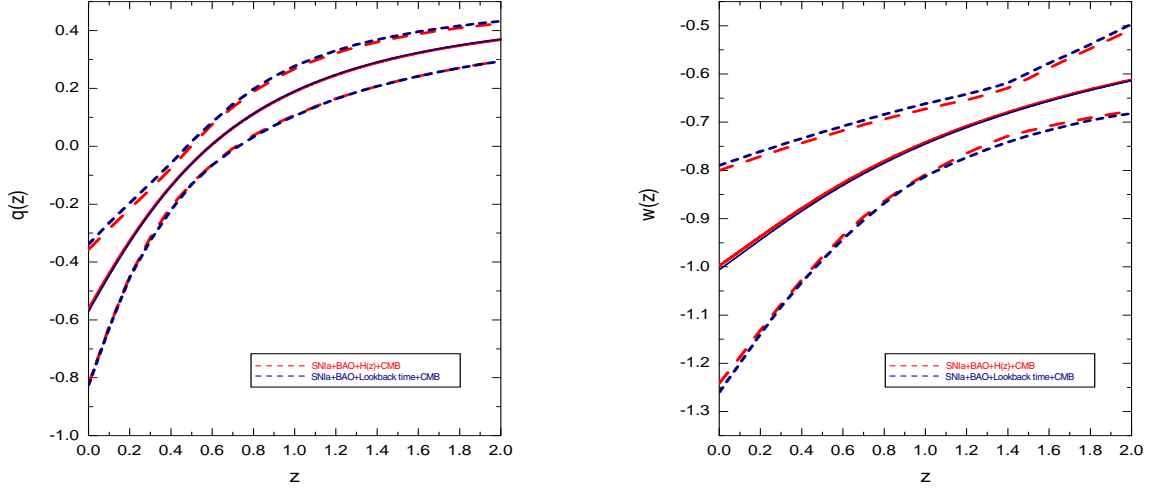
The up-to-date gold SN Ia sample was compiled by Riess et al [10]. This sample consists of 182 data, in which 16 points with $0.46 < z < 1.39$ were obtained recently by the Hubble Space Telescope (HST), 47 points with $0.25 < z < 0.96$ by the first year Supernova Legacy Survey (SNLS) and the remaining 119 points are old data. The SN Ia observation gives the distance modulus of a SN at the redshift z . The distance modulus is defined as

$$\mu_{th}(z; \mathbf{P}, \tilde{M}) = 5 \log_{10}(d_L(z)/\text{Mpc}) + 25 = 5 \log_{10}[(1+z) \int_0^z \frac{dz'}{E(z')}] + 25 - 5 \log_{10} H_0, \quad (7)$$

where the luminosity distance $d_L(z) = \frac{c(1+z)}{H_0} \int_0^z \frac{dz'}{E(z')}$, the nuisance parameter $\tilde{M} = 5 \log_{10} H_0$ is marginalized over by assuming a flat prior $P(H_0) = 1$ on H_0 , $\mathbf{P} \equiv \{c, \Omega_D, b^2\}$ describes a set of parameters characterizing the given model. In order to place constraints on the interacting holographic dark energy model, we perform χ^2 statistics for the model parameter \mathbf{P}

$$\chi_{SN}^2(\mathbf{P}, \tilde{M}) = \sum_i \frac{[\mu_{obs}(z_i) - \mu_{th}(z_i; \mathbf{P}, \tilde{M})]^2}{\sigma_i^2}. \quad (8)$$

Our analysis shows that if we use the SN Ia data, the constraint is not good, and the 1σ range is rather large.



(a) 1σ range of $q(z)$

(b) 1σ range of $w(z)$

Figure 7: (a) The evolution of $q(z)$ within the 1σ range. (b) The evolution of $w(z)$ within the 1σ range. The 1σ range of each combination is between the same colored dash lines. And the solid lines are the best-fit curves of each combinations.

An efficient way to reduce the degeneracies of the cosmological parameters is to use the SN Ia data in combination with the BAO measurement from SDSS [12] and the CMB shift parameter [11]. The acoustic signatures in the large scale clustering of galaxies yield additional test for cosmology. Using a large sample of 46748 luminous, red galaxies covering 3816 square degrees out to a redshift of $z = 0.47$ from the SDSS, Einstein et al [12] have found the model independent BAO measurement which is described by the A parameter

$$A = \sqrt{\Omega_m} E(z_{BAO})^{-1/3} \left[\frac{1}{z_{BAO}} \int_0^{z_{BAO}} \frac{dz'}{E(z')} \right]^{2/3} = 0.469 \left(\frac{n_s}{0.98} \right)^{-0.35} \pm 0.017, \quad (9)$$

where n_s can be taken as 0.95 [22] and $z_{BAO} = 0.35$. In our analysis we first investigated the joint statistics with the SN Ia data and the BAO measurement. The result is shown in Figure 1, where we show the contours of 68.3% , 95.4% and 99.7% confidence levels. The fitted parameters with the 1σ errors are shown in Table 1.

We also use the CMB shift parameter given by

$$R = \sqrt{\Omega_m} \int_0^{z_{ls}} \frac{dz'}{E(z')}, \quad (10)$$

where $z_{ls} = 1089$. This CMB shift parameter R captures how the l -space positions of the acoustic

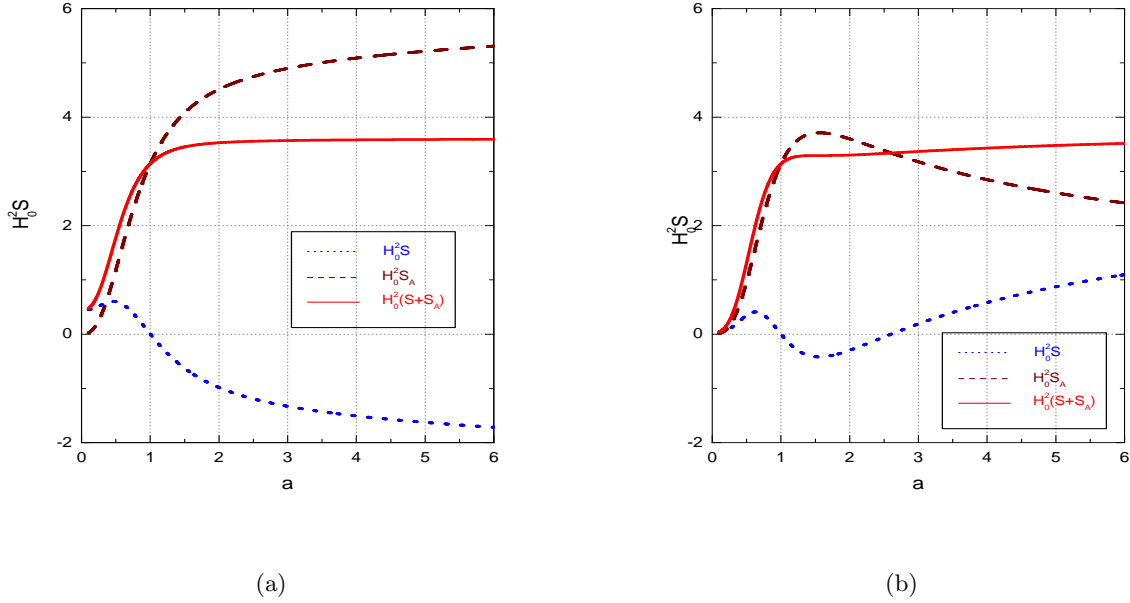


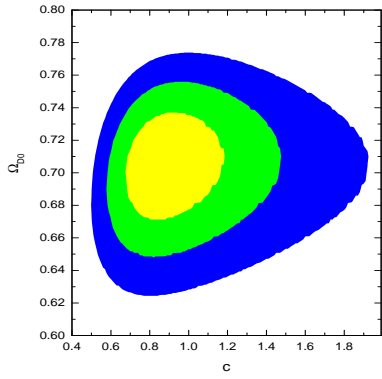
Figure 8: (a) The evolution of entropies with the $b^2 = 0.08$ and $c = 1$ and the initial conditions $\Omega_{D0} = 0.7$ and $H_0^2 S_0 = 10^{-30}$. (b) The evolution of entropies with the best fit parameters of the combination Lookbacktime+SN Ia+BAO+CMB, $b^2 = -0.003$ and $c = 0.83$ and the initial conditions $\Omega_{D0} = 0.71$ and $H_0^2 S_0 = 10^{-30}$.

peaks in the angular power spectrum shift. Its value is expected to be the least model independent and can be extracted from the CMB data. The WMAP3 data [22] gives $R = 1.70 \pm 0.03$ [11]. Now we can combine the SN Ia, WMAP3 and SDSS data to constrain the interacting holographic model. Using the χ^2 statistics, contours from the joint constraints SN Ia+BAO+CMB are shown in Figure 2. Comparing with Figure 1, we see that the errors have been reduced significantly in the joint analysis. The 1σ range of the model parameters are listed in Table 1 for comparison.

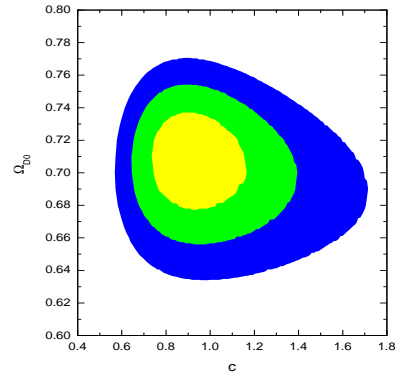
It is of interest to include the Hubble parameter data to constrain our model. The Hubble parameter depends on the differential age of the universe in terms of the redshift. In contrast to standard candle luminosity distances, the Hubble parameter is not integrated over. It persists fine structure which is highly degenerated in the luminosity distance [4]. Observed values of $H(z)$ can be used to place constraints on the models of the expansion history of the universe by minimizing the quantity

$$\chi_h^2(\mathbf{P}) = \sum_i \frac{[H_{obs}(z_i) - H_{th}(z_i; \mathbf{P})]^2}{\sigma_i^2}. \quad (11)$$

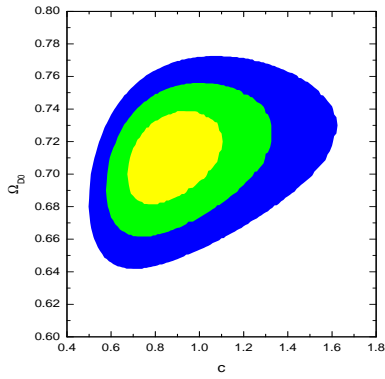
This test has been used to constrain several cosmological models [3, 4]. However this test on its own cannot provide tight constraint on the model. It is interesting to combine the $H(z)$ data with



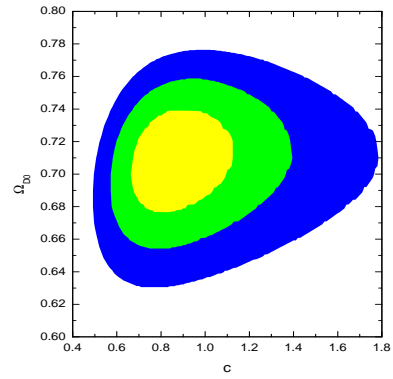
(a)SN Ia + BAO



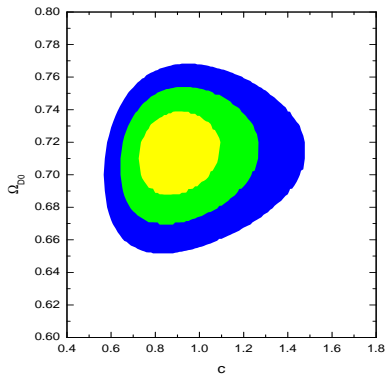
(b)SN Ia + BAO + CMB



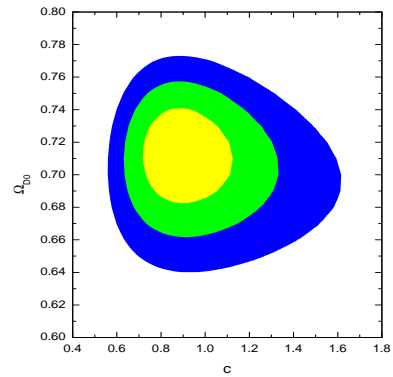
(c) $H(z)$ + SN Ia + BAO



(d)Lookback time + SN Ia + BAO



(e) $H(z)$ + SN Ia + BAO +CMB



(f)Lookback time + SN Ia + BAO +CMB

Figure 9: The contours in the holographic dark energy model without interaction. This graph shows observational contours in the $(c - \Omega_D)$ plane.

Table I: The best-fit data of the interacting holographic dark energy model.

	c	Ω_{D0}	b^2	χ^2_{min}
SNIa + BAO	$0.53^{+0.61}_{-0.22}$	$0.72^{+0.05}_{-0.04}$	$-0.10^{+0.131}_{-0.125}$	156.24
SNIa + BAO + CMB	$0.84^{+0.46}_{-0.25}$	$0.70^{+0.04}_{-0.04}$	$-0.004^{+0.012}_{-0.012}$	158.45
H(z) + SNIa + BAO	$0.82^{+0.89}_{-0.31}$	$0.71^{+0.05}_{-0.04}$	$-0.005^{+0.075}_{-0.075}$	167.74
Lookbacktime + SNIa + BAO	$0.62^{+1.22}_{-0.28}$	$0.72^{+0.05}_{-0.05}$	$-0.059^{+0.148}_{-0.126}$	159.48
H(z) + SNIa + BAO + CMB	$0.84^{+0.40}_{-0.25}$	$0.71^{+0.04}_{-0.04}$	$-0.003^{+0.010}_{-0.012}$	167.75
Lookbacktime + SNIa + BAO + CMB	$0.83^{+0.43}_{-0.25}$	$0.71^{+0.04}_{-0.04}$	$-0.003^{+0.012}_{-0.013}$	160.08

Table II: The best-fit data of the noninteracting holographic dark energy model.

	c	Ω_{D0}	χ^2_{min}
SNIa + BAO	$0.88^{+0.30}_{-0.20}$	$0.71^{+0.02}_{-0.03}$	158.54
SNIa + BAO + CMB	$0.91^{+0.25}_{-0.17}$	$0.71^{+0.02}_{-0.03}$	158.64
H(z) + SNIa + BAO	$0.85^{+0.26}_{-0.18}$	$0.71^{+0.02}_{-0.02}$	167.77
Lookbacktime + SNIa + BAO	$0.85^{+0.28}_{-0.18}$	$0.71^{+0.03}_{-0.03}$	160.14
H(z) + SNIa + BAO + CMB	$0.88^{+0.21}_{-0.15}$	$0.71^{+0.02}_{-0.02}$	167.96
Lookbacktime + SNIa + BAO + CMB	$0.89^{+0.23}_{-0.17}$	$0.71^{+0.03}_{-0.02}$	160.32

the data above to obtain tighter constraints on the interacting holographic dark energy model. The result on the joint analysis $H(z)$ +SN Ia+BAO is shown in Figure 3 and the 1σ ranges of different parameters are listed in Table I. Because the sample of $H(z)$ data is too small at this moment, the constraint on the model by including $H(z)$ data is not very tight. We hope that the future observations can offer more data of $H(z)$ so that χ^2 can be reduced. Adding the CMB shift parameter data, we have shown the combined analysis $H(z)$ +SN Ia+BAO+CMB shift in Figure 4. Comparing with Figure 3, it is interesting to notice that errors of model parameters have been significantly reduced.

Table III: The best-fit data of Λ CDM .

	Ω_{m0}	χ^2_{min}
SNIa + BAO	$0.30^{+0.02}_{-0.02}$	160.18
SNIa + BAO + CMB	$0.29^{+0.02}_{-0.02}$	161.85
H(z) + SNIa + BAO	$0.30^{+0.02}_{-0.02}$	169.22
Lookbacktime + SNIa + BAO	$0.30^{+0.02}_{-0.02}$	161.54
H(z) + SNIa + BAO + CMB	$0.29^{+0.02}_{-0.02}$	170.99
Lookbacktime + SNIa + BAO + CMB	$0.29^{+0.02}_{-0.02}$	163.05

The constraint based on SN Ia data and the recently proposed angular-redshift relation of compact radio sources are distance based methods to probe cosmological models, now we are going to test the model by using the time-dependent observable, the lookback time. The new test is expected to provide a complementary test of the model. This method has been employed in [6, 7, 9, 19]. The lookback time -redshift relation is defined by

$$t_L(z; \mathbf{P}) = H_0^{-1} \int_0^z \frac{dz'}{(1+z')E(z')}, \quad (12)$$

where $H_0^{-1} = 9.78h^{-1}$ Gyr, and we use the present value of $h = 0.72$ given by the HST key project [23], \mathbf{P} stands for the model parameters. To use the lookback time and the age of the universe to test a given cosmological model, let's follow [7] to consider an object i whose age $t_i(z)$ at redshift z is the difference between the age of the universe when it was born at redshift z_F and the universe age at z ,

$$t_i(z) = H_0^{-1} \left[\int_{z_i}^{\infty} \frac{dz'}{(1+z')E(z')} - \int_{z_F}^{\infty} \frac{dz'}{(1+z')E(z')} \right]. \quad (13)$$

Using the lookback time definition, we have $t(z_i) = t_L(z_F) - t_L(z)$. Thus the lookback time to an object at z_i can be expressed as

$$t_L^{obs}(z_i) = t_L(z_F) - t(z_i) = [t_o^{obs} - t_i(z)] - [t_o^{obs} - t_L(z_F)] = t_o^{obs} - t_i(z) - df, \quad (14)$$

where $df = t_o^{obs} - t_L(z_F)$ is the delay factor.

In order to estimate the parameters of our model, we minimize the χ^2 function

$$\chi_{age}^2(\mathbf{P}) = \sum_i \frac{[t_L(z_i; \mathbf{P}) - t_L^{obs}(z_i)]^2}{\sigma_i^2 + \sigma_{t_o^{obs}}^2} + \frac{[t_o(\mathbf{P}) - t_o^{obs}]^2}{\sigma_{t_o^{obs}}^2}, \quad (15)$$

where $\sigma_i = 1$ Gyr is the uncertainty in the individual lookback time to the i th galaxy cluster of our sample and $\sigma_{t_o^{obs}} = 1.4$ Gyr stands for the uncertainty on the total age of the universe until now. The current age of the universe in our analysis is taken as 14.4 Gyr. The second term in the χ^2 expression was introduced to make sure that the cosmological model can estimate the age of the universe at present in addition to describing the age of the universe at high redshift. Since the delay factor df does not appear explicitly in the theoretical value of $t_L(z_i)$, we will treat it as a nuisance parameter and marginalize it in our calculation. The joint statistical analysis of the combined observations including lookback time+SN Ia+BAO has been done and the result is shown in Figure 5. Comparing to the analysis of SN Ia+BAO shown in Figure 1, we noticed that the parameter space now is enlarged. This fact is expected and understood in term of the conservative uncertainty assumed ($\sigma_i = 1Gyr$) for the individual lookback time. In Figure 6, we

have shown the combined analysis including lookback time+SN Ia+BAO+CMB shift. It is easy to see that adding the CMB shift data, the model parameters have been constrained much tighter.

To illustrate the cosmological consequences led by the observational constraints, we show the evolution cases of the equation of state parameter $w(z)$ and the deceleration parameter $q(z)$ according to the best-fit values of our model parameters in Figure 7. It is easy to see that our model can have the feature of w crossing -1 . Our present equation of state and the deceleration parameter are consistent with CMB data [6, 22].

It is interesting to notice that our best fit value of b^2 , the coupling between dark energy and dark matter, is negative. In the holographic interacting dark energy model by employing the apparent horizon as the IR cutoff [20], it was argued that an equation of state of dark energy $w < 0$ is necessarily accompanied by the decay of the dark energy component into pressureless matter ($b^2 > 0$). However, in our model, negative b^2 can accommodate reasonable equation of state of dark energy which is clearly shown in the Figure 7. Another worry of the negative b^2 which implies a transfer of energy from the matter to the dark energy is that it might violate the second law of thermodynamics [21]. In order to check the second law of thermodynamics, we can employ the formula in [17]. Using the apparent horizon as a thermal boundary and evaluating the entropy inside the apparent horizon from the Gibbs law, we have shown the evolution of entropies in Figure 8. It is easy to see that for the best fit negative b^2 , entropy of matter and fluids inside the apparent horizon plus the entropy of the apparent horizon do not decrease with time. The generalized second law of thermodynamics is still respected.

For the sake of comparison, we have shown the same contours of the holographic dark energy model without interaction in Figure 9. And the best-fit results are shown in Table II. Combined SN Ia+CMB+BAO constraints on the holographic dark energy model without interaction have been studied in [24]. Here we have added the Hubble diagram data which is not an integrated over effect and the time-dependent observable analyses. Comparing with Figure 2, we find that $2\sigma, 3\sigma$ confidence ranges in the $c - \Omega_{D0}$ plane are much smaller for the holographic dark energy model without interaction. In the analysis we find that the difference between the model with and without interaction is bigger when the model parameter c is bigger. We have also listed the best-fit results for a flat Λ CDM model in Table III. At the first glance, from the χ^2_{min} , it gives us a sense that the interaction between dark energy and dark matter gives a better description of the combined observations although this interaction is extremely small. Considering the additional degree of freedom, it is still early to say that our interacting holographic dark energy model is more favored than the Λ CDM model. However one advantage of the interacting holographic model is

that, unlike the Λ CDM model, it can alleviate the coincidence problem[6, 16].

In summary, in this work we have performed a parameter estimation of the interacting holographic dark energy model which could explain the observed acceleration of our universe. We have analyzed data coming from the most recent SN Ia samples, CMB shift, LSS observation, $H(z)$ and lookback time measurements. Comparing with the single observational test, we learnt that the joint analysis of different observations based on different observables is powerful to overcome the statistical uncertainties. We have got useful consistent check of the interacting holographic dark energy model and tighter constraints on the model parameters. The joint analysis indicates that this is a viable model. In the 1σ range, it can explain the transition of the equation of state from $w > -1$ to $w < -1$. It is worth noting that although the current $H(z)$ and lookback time data do not provide very restrictive constraints, richer samples of $H(z)$ data and more precise age measurements of high- z objects will provide a complementary check of the cosmic acceleration model. The joint statistical analysis is necessary to test the model.

We observed that the best fit coupling between dark energy and dark matter is negative, which indicates that there is a possible energy transfer from the matter to the dark energy. Although the generalized second law of thermodynamics is shown not threatened by the best fit negative b^2 , the holographic principle might still violate in the future if there is a continuing energy transfer from the matter to the dark energy, since in the late stage it is possible to see that $S < S_A$ in Figure 8. In view of the unknown nature of dark energy and dark matter, we can't say for certain the direction of the energy transfer between dark energy and dark matter. However from the observation data and the holographic principle requirement, the nature thing we can learn is that in the past there is an energy flow from the matter to the dark energy from the observational data, while in the future there requires an energy transfer from the dark energy to the matter to satisfy the holographic principle. A nature description of the coupling between dark energy and dark matter is called for, which is important to influence the structure formation and the description of the universe evolution.

Acknowledgments

This work was partially supported by NNSF of China, Ministry of Education of China and Shanghai Educational Commission. Y.G.G. was supported by Baylor University, NNSFC under Grants No. 10447008 and No. 10605042, CMEC under Grant No. KJ060502, and SRF for ROCS,

State Education Ministry. B. W. would like to acknowledge helpful discussions with D. Pavon.

- [1] A.G. Riess *et al.*, *Astron. J.* **116**, 1009 (1998); S. Perlmutter *et al.*, *Astrophys. J.* **517**, 565 (1999).
- [2] J. Simon, L. Verde and R. Jimenez, *Phys. Rev. D* **71**, 123001 (2005).
- [3] L. Samushia and B. Ratra, *Astrophys. J.* **650** (2006) L5; R. Lazkoz, E. Majerotto, arXiv:0704.2606.
- [4] H. Wei and S. N. Zhang, arXiv:astro-ph/0609597. P. Wu and H. W. Yu, *Phys. Lett. B* **644** (2007) 16 [arXiv:gr-qc/0612055]. P. X. Wu and H. W. Yu, arXiv:astro-ph/0701446. L. I. Xu, C. W. Zhang, B. R. Chang and H. Y. Liu, arXiv:astro-ph/0701519. A. Kurek and M. Szydlowski, arXiv:astro-ph/0702484. H. Zhang and Z. H. Zhu, arXiv:astro-ph/0703245.
- [5] A. Friaca, J. S. Alcaniz, J. A. S. Lima, *Mon. Not. Roy. Astron. Soc.* **362** (2005) 1295.
- [6] B. Wang, J. D. Zang, C. Y. Lin, E. Abdalla, S. Micheletti, astro-ph/0607126, *Nucl. Phys. B*(in press).
- [7] S. Capozziello, V.F. Cardone, M. Funaro and S. Andreon, *Phys.Rev. D***70**, 123501 (2004).
- [8] A. Sandage, *Ann. Rev. Astron. Astrophys.* **26**, 561 (1988).
- [9] N. Pires, Z. H. Zhu, J.S. Alcaniz, *Phys.Rev. D***73** (2006) 123530.
- [10] A. G. Riess, et al. 2006, *ApJ*, accepted (astro-ph/0611572)
- [11] Y. Wang, P. Mukherjee, 2006, *ApJ*, **650**, 1; astro-ph/0703780.
- [12] D. J. Eisenstein, et al. 2005, *ApJ*, **633**, 560.
- [13] B. Wang, Y. G. Gong, E. Abdalla, *Phys. Lett. B.* **624** (2005) 141
- [14] B. Wang, C. Y. Lin, E. Abdalla, *Phys. Lett. B.* (in press), hep-th/0509107
- [15] R. Caldwell, M. Doran, *Phys. Rev. D* **69** (2004), 103517; U. Alam, V. Sahni, A. A. Starobinsky, *JCAP* **0406** (2004) 008; D. Huterer, A. Cooray, *Phys. Rev. D***71** (2005) 023506; Y.G. Gong, *Class. Quantum Grav.* **22** (2005) 2121; Y. Wang, M. Tegmark, astro-ph/0501351; H.K.Jassal, J.S.Bagla, T. Padmanabhan *Phys. Rev. D***72** (2005) 103503, astro-ph/0506748.
- [16] L. Amendola *Phys. Rev. D***62** (2000) 043511; Havard Sandvik, Max Tegmark, Matias Zaldarriaga and Ioav Waga *Phys. Rev. D***69** (2004) 123524, astro-ph/0212114.
- [17] B. Wang, Y. G. Gong, E. Abdalla, *Phys.Rev. D***74** (2006) 083520.
- [18] Q. Wu, Y. G. Gong, A. Z. Wang, J.S. Alcaniz, arXiv:0705.1006.
- [19] M. Li, *Phys. Lett. B* **603** (2004) 1; Q.G. Huang and M. Li, *JCAP* **0408** (2004) 013.
- [20] D. Pavon and W. Zimdahl, *Phys. Lett. B***628** (2005) 206, gr-qc/0505020.
- [21] G. Olivares, F. A. Barandela and D. Pavon, *Phys. Rev. D* **71**, 063523 (2005); S. D. Campo, R. Herrera and D. Pavon, *Phys. Rev. D* **71**, 123529 (2005).
- [22] D. N. Spergel et al., astro-ph/0603449.
- [23] W.L. Freedman et al., *Astrophys. J* **553** (2001) 47.
- [24] X. Zhang, F. Q. Wu, astro-ph/0701405.